scientific reports



OPEN Optimal fuzzy-PID controller design for object tracking

Yaregal Limenih Melese¹, Girma Kassa Alitasb² & Mequanent Degu Belete²

Object tracking is a technique for finding moving objects of interest and estimating their trajectory or path with regard to time in a series of images. It involves object representation, detection, and tracking. It becomes an important field of study due to the need in video surveillance, traffic monitoring, live sport video analysis and many other applications. In this paper, both static camerabased and dynamic camera-based object tracking techniques have been developed. The static camerabased object tracking was developed with NI LabVIEW, and Shape adaptive mean-shift algorithm has been used for tracking. In case of dynamic camera-based object tracking, an optimal Fuzzy-PID controller has been designed to adjust the position of the pan/tilt mechanism so as to trace the object's trajectory. Genetic algorithm (GA) was used to find the optimal values of the operating ranges (scaling factors) of the membership functions. The performance of the system has been tested by different trajectories like step, sinusoidal, circular and elliptical at different frequencies 1, 50 and 100 rad/sec. The system has best performance at low frequencies and when the frequency or speed of the object increases, the system performance decreases which complies for real systems. The simulation results demonstrate that GA tuned Fuzzy-PID controller has given us the best results in terms of reduced steady-state error, faster rise time and settling time, and object position stabilization than PID, Fuzzy and Fuzzy-PID controllers, which shows that optimal Fuzzy-PID controller designed is more appropriate and efficient.

Keywords Object tracking, LabVIEW, Fuzzy-PID, Pan/Tilt system, Genetic algorithm

Humans and animals need to observe the changing nature of their surroundings^{1,2}. They sense and multiply environmental changes using physiological systems implanted in their bodies. The five sense organs used by animals to understand the scene and take the right actions to reach their goals are sight, hearing, touch, smell, and taste. Animals other than humans (non-rational animals) intentions are just simple and limited to safety, chasing for food and defense. But humans have a high level of understanding and are capable of interpreting the changes happening in the environment, adding knowledge, and think forward to do in advance for future behaviors 1,3,4.

Interest object detection and tracking are significant researches in the field of computer vision^{5–7}. Computer vision⁸ is the study of allowing computers to see, recognize, and interact with the world in the same way that humans do. In order to understand and cooperate with the world, computers must be capable of locating objects of interest and continuously following these objects, a task known as visual tracking, which is also at the heart of numerous computer vision applications such as surveillance, robotic, and monitoring applications⁴.

Object tracking, the main objective of this paper, is the method of locating a moving object (or several ones) and estimating its course along time in a sequence of images. It comprises two steps: detection of interest objects and traces their trajectories. Furthermore, object tracking could also involve behavior analysis, object and activity classification, specific person identification, counting, flux statistics, and alarming9. Tracking3 is the way of locating a moving object or multiple objects over a period of time with a camera. Object tracking is technically a problem of reckoning object paths in image planes while moving around a scene.

Tracking can be seen as the main task involving several subtasks such as image segmentation for object detection, object matching, and position estimation. Lots of tracking algorithms have been established to implement and solve these subtasks. But each of the algorithms has its strengths and weaknesses. To find an optimal tracking system for a certain kind of application, extensive researches have been conducted in this field over the last years. Despite the fact that various object-tracking strategies have been put forth in a number of literary works over the past several years, but it is not common to have both the detection and tracking parts covered together and the results are scene specific. Good results are dependent on a certain number of assumption verifications and the quality of the devices and tools used for the tracking purpose^{1,10,11}. The motivation for this

¹Faculty of Electrical and Computer Engineering, Bahir Dar Institute of Technology, Bahir Dar University, Bahir Dar, Ethiopia. ²School of Electrical and Computer Engineering, Debre Markos Institute of Technology, Debre Markos University, Debre Markos, Ethiopia. [™]email: girma_kassa@dmu.edu.et

paper is to implement genetic algorithm tuned Fuzzy-PID controller and shape adaptive mean shift algorithm, to improve the detection and tracking process.

LabVIEW, a graphical programming language first brought up for the Apple Macintosh in 1986, is being utilized for many applications like computer vision, data acquisition, industrial automation, instrumental control, and different computations^{2,5,6,12}. Image processing using LabVIEW gives better results. It takes place with block representations and becomes simpler than writing complicated programming. Object tracking, pattern matching, edge detection, and histogram, etc. can be easily done using the NI-LabVIEW and NI-Vision Assistant^{2,10}.

It is not common in most researches to have both the detection and tracking techniques delt together. In the detection phase, researchers write a complex algorithm in MATLAB, Python and OpenCV $^{13-15}$. However, as complexity increases the processing time increases drastically and this in turn decreases the efficiency of our work. Researches try to use different tracking approaches too. Nevertheless, the results they obtain still need some improvements especially in real time applications. Here is a look at some groundbreaking researches that was recently completed.

A study¹⁶ proposed a novel control methodology that combines Genetic Algorithms (GA) with fuzzy PID control to improve the energy efficiency of dynamic energy systems. This approach utilizes GA to optimize the design of the fuzzy controller, leading to superior performance with minimal settling time and no overshoot or undershoot. However, the paper lacks details on the specific parameters optimized by the GA and numerical data on the system's transient and steady-state behavior.

In¹⁷ an effective control design approach based on novel enhanced aquila optimizer for automatic voltage regulator has been discussed. Enhanced Aquila Optimizer (enAO) is a modified version of the Aquila Optimizer (AO). The performance of the proposed enAO algorithm has been integrated with PIDD² controller and they showed that the results outperform the other controller and optimization algorithms. But they did not mention about the GA and the transient and frequency response figures are still need an improvement.

Artificial ecosystem-based optimization integrated with Nelder-Mead method have been employed for PID controller design of buck convertor¹⁸. The researchers have demonstrated that the effectiveness of the proposed algorithm over AEO, PSO, And DE. They also stated that in terms of the transient and steady state response characteristics, the performance of the proposed algorithm is superior.

Atom search optimization and particle swarm optimization have been used to create a hybrid algorithm called hybrid atom search particle swarm optimization (h-ASPSO) for high order systems in 19. Improved time domain performance of high order engineering systems has been stated in this research. The performance of the proposed optimization technique has been compared with the other available techniques based on genetic algorithm, symbiotic organisms search algorithm, many optimizing liaisons algorithm and atom search optimization algorithm.

In²⁰ Augmented hunger games search algorithm using logarithmic spiral opposition-based learning for function optimization and controller design have been discussed. The proposed algorithm has been used as an efficient tool for both optimization and controller design for the magnetic ball suspension system.

To enhance the effectiveness of car antilock braking systems in the presence of uncertainty²¹, developed an indirect exponential sliding-mode controller based on the interval type-2 fuzzy neural network. The findings of this study confirm that the planned approach significantly enhances the control performance of vehicle antilock braking systems²². suggested a type-2 fuzzy neural network-based adaptive control method that is both robust and adaptive for tracking a quadrotor's planned position and orientation trajectories. The cuckoo optimization technique is used in this work to optimize the parameters of the sliding mode controller.

The authors in²³ have proposed a novel improved version of hunger games search algorithm for function optimization and efficient controller design of buck converter system. The proposed method has been comparatively demonstrated as more efficient design approach to tune the FOPID controlled buck converter system.

The studies mentioned above and many more investigated various optimization algorithms for different applications. Unfortunately, there is no single best optimization technique that works for all scenarios. The optimal choice depends heavily on the specific problem we are trying to solve. GA is considered to be a matured optimization technique as it has a long history and widespread adoption. Its extensive use indicates its effectiveness in various domains.

Not a one-size-fits-all solution. GAs, like most optimization techniques, have limitations. They might struggle with highly complex problems or require careful parameter tuning to achieve optimal performance. While the core principles are established, research on GAs continues. This includes exploring new variations, hybridization with other techniques, and improving their efficiency for specific problem types.

This paper combines two key areas: object detection and control techniques. Below are the summaries of the contributions of the paper:

- The integration of object detection with an optimal fuzzy-PID controller for tracking. This would be a beneficial for real world applications where precise control of a moving object is required based on real time detections.
- Optimal fuzzy-PID controller design by employing GA. Actually, GA, PSO or enAO can be used as optimization algorithms in order to find the best parameters required.
- The paper demonstrates an improved tracking performance compared to the conventional PID, Fuzzy Logic, Fuzzy-PID, and GA tuned/optimized PID controllers. This has been evaluated by the transient and steady state response characteristics.
- In general, the paper contributes an efficient and robust object tracking solution by combining object detection with an optimized fuzzy-PID controller.

System description and methodology

The proposed object tracking system comprises of a camera for object vision, two servo motors to perform high accuracy positioning system (pan and tilt mechanism). It additionally has a regulator to efficiently follow the object under the scene by changing the position of the servo motors with a feedback system. The camera is mounted to the pan motor shaft, and the tilt motor is attached in a manner to give a tilt move for the camera and pan motor configuration. Thus, we can pan and tilt the camera field of view. The resolution of each frame from the camera is taken to be (640, 480), and the pixel point (320, 240) is the center point of the camera. The tracked object center location (a, b) is needed to be maintained at the center point of the camera (320, 240). The coordinate system from captured frame and the block diagram of the object tracking system are given in Figs. 1 and 2.

In Fig. 2 an image processing system first determines the camera's position by analyzing the captured image. This information is then fed back to the processing tool. The tool compares the extracted camera position (actual position) with a set of desired positions. This difference, often called the "position error," is then sent to a controller. The controller uses this error signal to adjust the pan-tilt mechanism, aiming to minimize the difference and move the camera towards the desired position.

Additionally, a disturbance, such as wind or an unexpected object bump, have been introduced at the input of the pan-tilt system. This disturbance can cause the camera to deviate from its intended path.

Object tracking in LabVIEW

Object detection is locating inters objects in the frame of a video sequence and every object tracking algorithm needs an object detection system either in each frame of a video sequence or when the object first appears in the video 15.

The tracking process uses three main steps, detection of interest objects, tracking of these objects, and examination of these objects to understand and interpret their behavior. Interest objects can be represented in their shape or appearance²⁴.

The methodology employed to detect and track objects in LabVIEW is given in Fig. 3 below. In order to follow the object of interest, the camera needs to be interfaced with a PC.

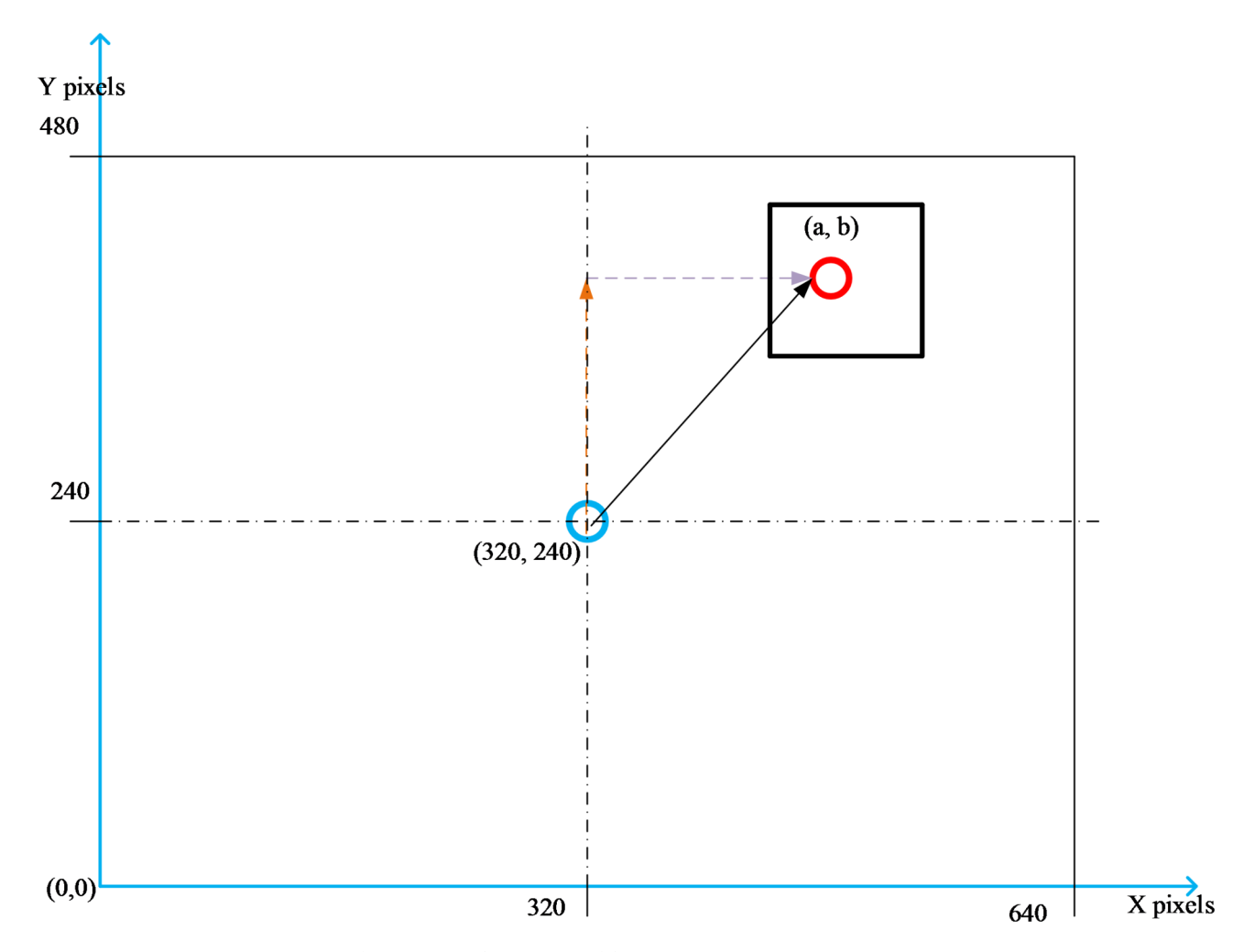


Fig. 1. Coordinate system from captured frame.

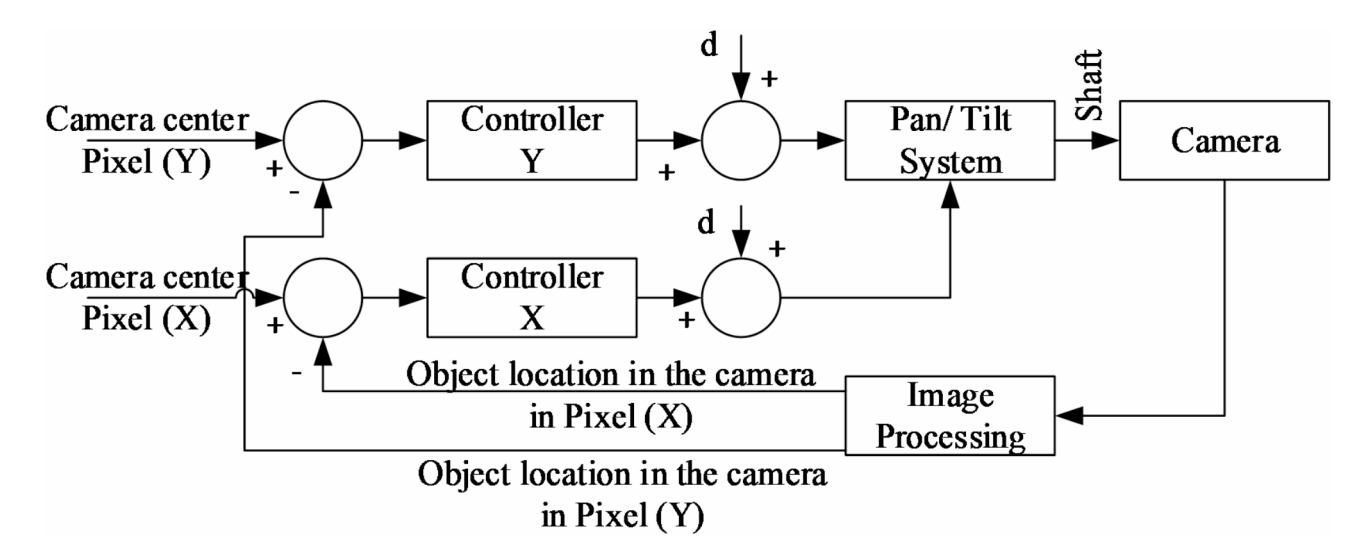


Fig. 2. Block diagram of object tracking system connections.

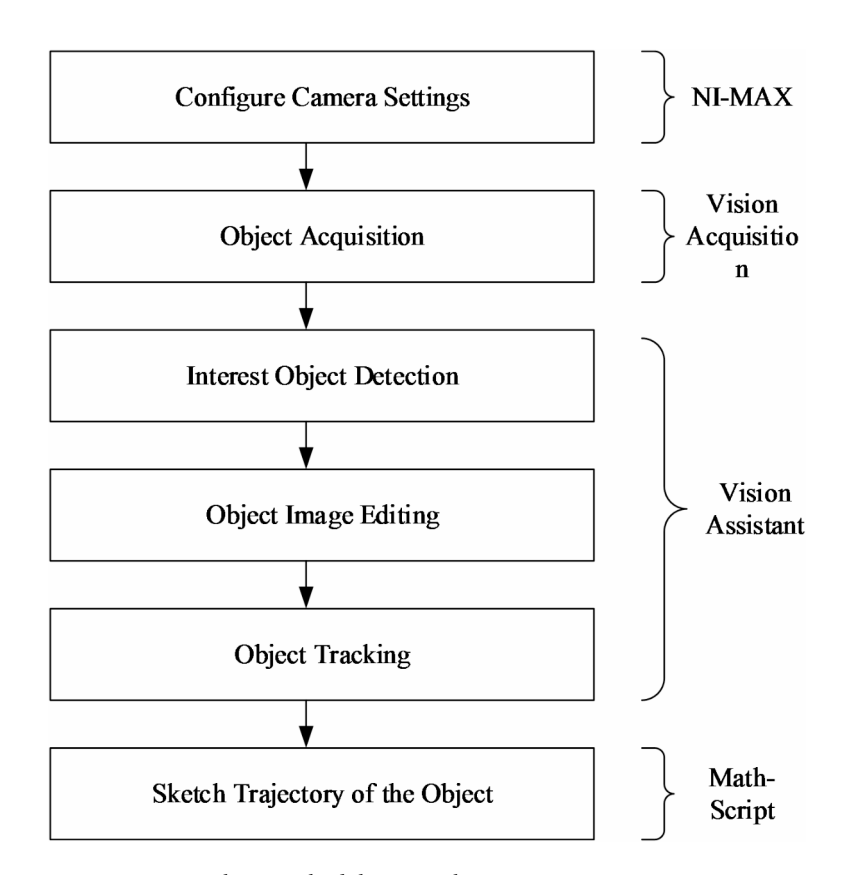


Fig. 3. Image tracking methodology in LabVIEW.

The NI-MAX (National Instruments Measurement and Automation Explorer) is used to configure the camera and all the settings required for the tracking purpose. After an appropriate configuration of the camera, the next step is image acquisition and this is done with use of NI Vision Acquisition Express. There are some configuration settings like acquisition type (continuous acquisition with inline processing used in this work), and acquisition configuration settings like contrast, brightness, saturation, sharpness etc. An adjustment has been made until the better images of the object are acquired²⁴.

The images acquired in this step are then feed to the NI Vision Assistant for further processing. The gray scale images are used over RGB color images in order to get a better efficiency due to reason that color images let the display respond slowly specially at higher resolutions. The block diagram of the object detection and tracking procedure employed in LabVIEW is given in Fig. 4.

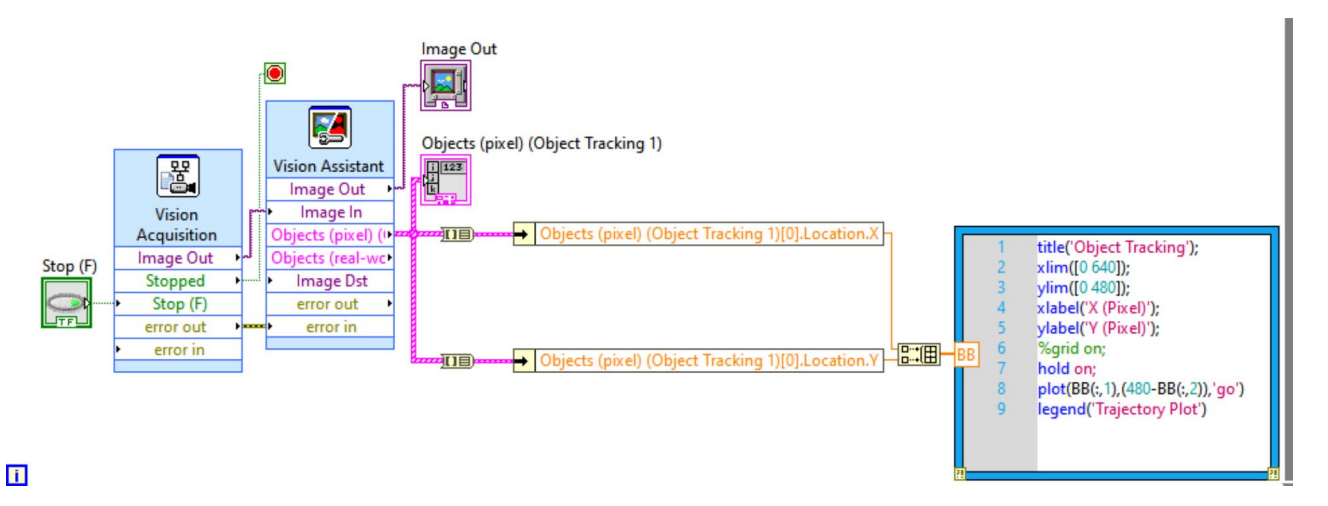


Fig. 4. Block diagram of object detection and tracking in LabVIEW.

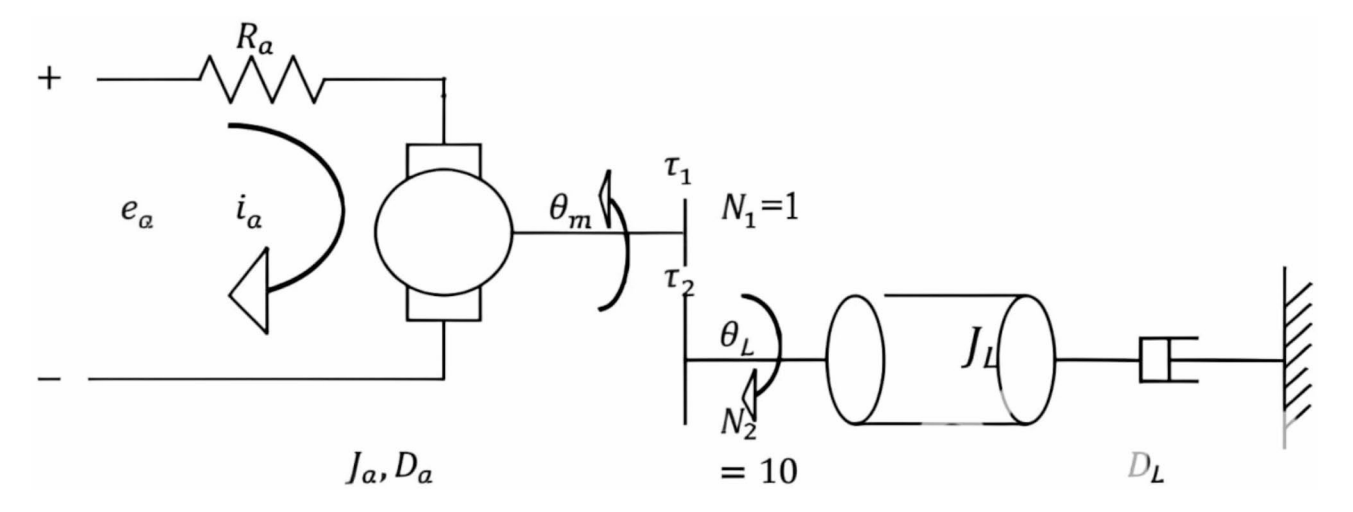


Fig. 5. The equivalent circuit representation of DC servomotor and gear load²⁶.

The shape adaptive kernel based mean shift algorithm has been used for tracking as it has the ability to track objects that may appear to change in size or shape. Math-Script module has been used to sketch the trajectory of the object.

Pan/Tilt mechanism model

The pan and tilt mechanism of the tracking system can be modeled as two separate actuators²⁵. The one actuator corresponds to the pan movement, and the other one corresponds to the tilt movement of the camera. The camera captures the interest object with the help of NI-Vision and after some image processing techniques, we extract the object's x and y location on the captured frame. These object locations in a 2-D plane are then feedbacked to the controller as a reference in order to control the position of the actuators efficiently. Separately excited armature-controlled DC servomotor is used in this work. The equivalent circuit of this motor is given in Fig. 5²⁶.

The core equations that represent the armature-controlled DC servomotor are given below: Torque Eq.

$$T_M = K_T I_a \tag{1}$$

Where K_T is the given motor torque constant in (N-m/A) and I_a is the armsture current in (A). Electrical and mechanical Eq.

$$L_a \frac{di_a}{dt} + R_a I_a = V_a - K_b \, \omega \tag{2}$$

$$J\frac{d\omega}{dt} + D\omega = K_T I_a - T_w \tag{3}$$

Where V_a , T_w , J and D are the applied armature voltage in volts, the disturbance torque in Newton-meter (N-m), Moment of Inertia (Kg- m^2) and Viscous-friction coefficient (N-m/KRPM) respectively.

In our case, the DC motor shaft is attached to a gearbox with ratio ($K_g = \frac{N_l}{N_m}$), (where N_l and N_m are the number of teeth on the load side and the number of teeth on the motor side respectively), and then the camera is attached to the output shaft of the gearbox. The gear ratio relates motor shaft angular position θ_m to the load shaft angular position θ_l as $K_g = \frac{\theta_m}{\theta_l}$). The load inertia J_l acting at the output shaft of the gearbox reflected to the motor shaft side is given by $\frac{1}{K_g^2}J_l$. As torque is utilized to drive the motor shaft and the camera load attached, the torque equation in Eq. (3) above can be rewritten as below assuming no disturbance torque²⁷:

$$T_M = K_T I_a = J_m \frac{d^2 \theta_m}{dt^2} + \frac{1}{K_a^2} J_l \frac{d^2 \theta_m}{dt^2} + \frac{1}{K_a^2} D \frac{d\theta_m}{dt}$$
 (4)

$$T_M K_g = J_{eq} \frac{d^2 \theta_l}{dt^2} + D \frac{d\theta_l}{dt}$$
 (5)

Where, $J_{eq} = J_m K_g^2 + J_l$, is the total load inertia reflected at the motor shaft and D is the rotational viscous friction constant. Taking the Laplace Transform of Eq. (4), the below equation is obtained:

$$T_{M}\left(s\right) = J_{m}s^{2}\theta_{m}\left(s\right) + \frac{1}{K_{q}^{2}}J_{l}s^{2}\theta_{m}\left(s\right) + \frac{1}{K_{q}^{2}}Ds\theta_{m}\left(s\right)$$

$$\tag{6}$$

After having some algebraic manipulations, the equations relating $\theta_m(s)$ with $V_a(s)$ and $\theta_l(s)$ with $V_a(s)$ are given below:

$$\frac{\theta_m(s)}{V_a(s)} = \frac{K_g^2 K_T}{L_a J_{eq} s^3 + (L_a D + R_a J_{eq}) s^2 + (R_a D + K_g^2 K_T K_b) s} = T \tag{7}$$

$$\frac{\theta_{l}(s)}{V_{a}(s)} = \frac{K_{g}K_{T}}{L_{a}J_{eq}s^{3} + (L_{a}D + R_{a}J_{eq})s^{2} + (R_{a}D + K_{g}^{2}K_{T}K_{b})s}$$
(8)

The block diagram representation of the motor and the load together with the gear is presented in Fig. 6 below. The transfer function from the input voltage V_a (s) to the load shaft angular velocity ω_l (s) is given by:

$$\frac{\omega_{l}(s)}{V_{a}(s)} = \frac{K_{g}K_{T}}{L_{a}J_{ea}s^{2} + (L_{a}D + R_{a}J_{ea})s + (R_{a}D + K_{a}^{2}K_{T}K_{b})}$$
(9)

As the characteristic equation is a second order, take two simple real roots as r_E and r_M . Applying partial fraction expansion to Eq. (9) above the below equation is obtained:

$$\frac{\omega_l(s)}{V_a(s)} = \frac{A_E}{s + r_E} + \frac{A_M}{s + r_M}$$
(10)

Closed-loop position control of servomotors.

The new transfer function, obtained from Eq. (10) by neglecting the electrical component (as in most practical armature-controlled DC servomotor applications, $r_E >> r_M$ and this lets the electrical subsystem respond well faster than the mechanical subsystem), relating the output shaft angular position to the input voltage is given below:

$$\frac{\theta_l(s)}{V_a(s)} = \frac{A_M}{s(s+r_M)} \tag{11}$$

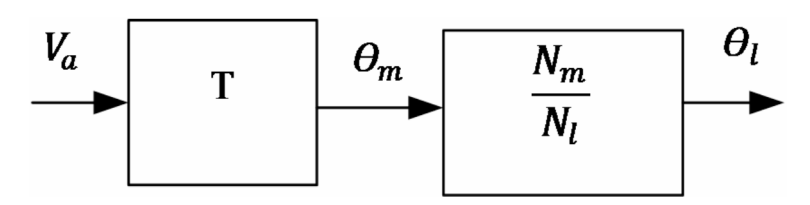


Fig. 6. Representation of the transfer function between load angle (angle at secondary gear) and armature voltage.

The DC motor load angular velocity response, $\omega_l(s)$, to the armature voltage input, $V_a(s)$, transfer function given in Eq. (9) above can be approximated by a first-order transfer function model, and is given below²⁷:

$$\frac{\omega_l(s)}{V_a(s)} = \frac{K_g K_T}{J_{ea}R_a s + (DR_a + K_a^2 K_T K_b)}$$
(12)

The s- domain unit step response of the output angular position is:

$$\theta_l(s) = \frac{A_M}{s(s+r_M)} \frac{1}{s} \tag{13}$$

The final value of the response by employing final value theorem is given by:

$$\lim_{t \to \infty} \theta_o(t) = \lim_{s \to 0} s \theta_l(s) = \lim_{s \to 0} s \left(\frac{A_M}{s(s + r_M)} \frac{1}{s} \right) = \infty$$
 (14)

As seen from Eq. (14) above, the final value of the response is unbounded and hence in order to control the output position follow the input position command, the output position is feedback to the input and this insures it. Considering only a proportional control, the equation for the control unit is given below^{27,28}:

$$V_a(s) = K_p \left[\theta_i(s) - \theta_l(s) \right] \tag{15}$$

From Eq. (11) above we have:

$$V_a(s) = \frac{s(s+r_M)}{A_M}\theta_l(s)$$
(16)

Then the block diagram showing the servo motor position control using position feedback is given in Fig. 7. The transfer function relating $\theta_l(s)$ to $\theta_i(s)$ is given as follows:

$$\frac{\theta_l(s)}{\theta_i(s)} = \frac{A_M K_p}{s^2 + r_M s + A_M K_p} \tag{17}$$

Equating Eqs. (10) and (12) above and with some rearrangement A_M and r_M can be given as:

$$A_M = \frac{?_g K_g K_T}{R_a J_{eq}} \tag{18}$$

$$r_M = \frac{DR_a + ?_g K_g^2 K_T K_b}{R_a J_{eq}}$$
 (19)

Where, $?_g$, is the motor gear box efficiency.

Using parameters obtained from servomotor vendor (SANYO DENKI), the specifications of DC servo motors employed in the modeling process are presented in Table 1 below.

The elevation and azimuth actuator transfer functions are then obtained by employing Eqs. (18) and (19) as follows:

For x-motor (azimuth):

$$A_M = \frac{\eta_g K_g K_T}{R_a J_{eq}} = 204.92 \tag{20}$$

$$r_M = \frac{DR_a + \eta_g K_g^2 K_T K_b}{R_a J_{eq}} = 135.01$$
 (21)

$$\frac{\theta_l(s)}{\theta_i(s)} = \frac{204.92K_p}{s^2 + 135.01s + 204.926K_p} = \frac{204.92}{s^2 + 135.01s + 204.92}$$
(22)

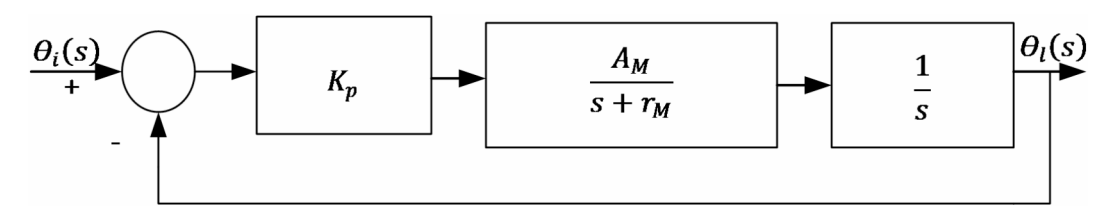


Fig. 7. Servo motor position control using position feedback.

Parameter	Definition	y-motor (elevation)	x-motor (azimuth)
P_R	Rated output power (W)	80	60
V_R	Rated armature voltage (V)	24	24
T_R	Rated torque (Nm)	0.26	0.19
I_R	Rated armature current (A)	5.0	3.9
N_R	Rated speed (rpm)	3000	3000
T_s	Continuous stall torque (Nm)	0.32	0.24
T_P	Peak stall torque (Nm)	2.16	1.8
I_s	Armature stall current (A)	5.2	4.5
I_p	Peak armature stall current (A)	40	31
Q_R	Rated power rate (kW/s)	1.8	1.6
K_T	Torque constant (Nm/A)	0.06	0.057
K_b	Back EMF constant (Vs/rad)	0.66 x 10 ⁻³	0.63 x 10 ⁻³
J_{eq}	Rotor inertia (kg m^2)	0.37 x 10 ⁻⁴	0.22×10^{-4}
D	Damping constant (Nms/rad)	8.22x 10 ⁻³	2.97x 10 ⁻³
R_a	Armature winding resistance (Ω)	0.44	1.1
L_a	Armature inductance (mH)	0.3	0.5
τ m	Mechanical time constant (ms)	4.5	7.4
τ e	Electrical time constant (ms)	0.61	0.45
K_g	Gear ratio	0.1	0.1
?g	Motor efficiency	0.87	0.87

Table 1. Specifications of DC servo motor.

$$A_M = \frac{\eta_g K_g K_T}{R_a J_{eq}} = 320.64 \tag{23}$$

$$r_M = \frac{DR_a + \eta_g K_g^2 K_T K_b}{R_a J_{eg}} = 222.18$$
 (24)

$$r_{M} = \frac{DR_{a} + \eta_{g}K_{g}^{2} K_{T} K_{b}}{R_{a}J_{eq}} = 222.18$$

$$\frac{\theta_{l}(s)}{\theta_{i}(s)} = \frac{320.64K_{p}}{s^{2} + 222.18s + 320.64K_{p}} = \frac{320.64}{s^{2} + 222.18s + 320.64}$$
(25)

Designed GA optimized fuzzy PID controller

As the non-linearity and complexity of the system increases, the conventional PID and Fuzzy logic controllers fail to give efficient results. It is appropriate to use genetic algorithm tuned fuzzy-PID controller in order to improve control performance, reduced settling time, overshoot and steady state error. The systems adaptability to changing system dynamics also increases.

Having obtained the pan/ tilt mechanism model's transfer function for positioning the camera, an optimal Fuzzy PID controller has been designed that controls the servomotors in a two-dimensional coordinate plane. Genetic algorithm was used to tune the operating ranges of the membership functions for the Fuzzy-PID controller.

The following configurations were used to optimize the system parameters using the genetic algorithm. The number of possible solutions assessed in each generation was represented by the population size, which was set at 30. This size was selected to achieve a balance between the algorithm's effective research of the solution space and computational efficiency. Three variables, each encoded as a gene within a chromosome, were part of the optimization problem. The system performance was evaluated using the Integral of Time-weighted Absolute Error (ITAE) as the objective function. Because ITAE reduces time-weighted error, it is especially well-suited for control system applications where speed and precision are crucial. In order to guarantee that 20% of the fittest individuals from each generation were kept for the following iteration, a reproduction rate of 0.2 was chosen. This method enhances genetic variety while preserving the quality of the solutions. A crossover rate of 0.8 was applied, meaning 80% of the population underwent crossover operations to produce offspring. This high rate promotes integrating features from parent chromosomes to explore the solution space. To ensure diversity within the population and avoid early convergence, 5% of the population was randomly modified at a mutation rate of 0.05. A maximum of 30 iterations were used in the optimization procedure because early tests showed that this was enough to reach convergence. The GA parameters used in the simulation are summarized in Table 2.

Regarding the optimization process, each chromosome represents a potential solution to the optimization problem, and the process starts by producing an initial population of 30 candidate solutions. To evaluate each chromosome's fitness and make selections for reproduction, the ITAE objective function is used. With a probability of 0.8, chosen chromosomes undergo crossover to create new offspring. To increase diversity, 5% of the population is subjected to a mutation which introduces random gene modifications. At iteration 30, the optimization process reached at its optimal solution.

No.	Design parameter	Value
1	Population size	30
2	Number of variables	3
3	Optimization function	ITAE
4	Reproduction rate	0.2
5	Crossover rate	0.8
6	Mutation rate	0.05
7	Maximum iteration	30

Table 2. Selected design parameters for GA based Fuzzy-PID optimization.

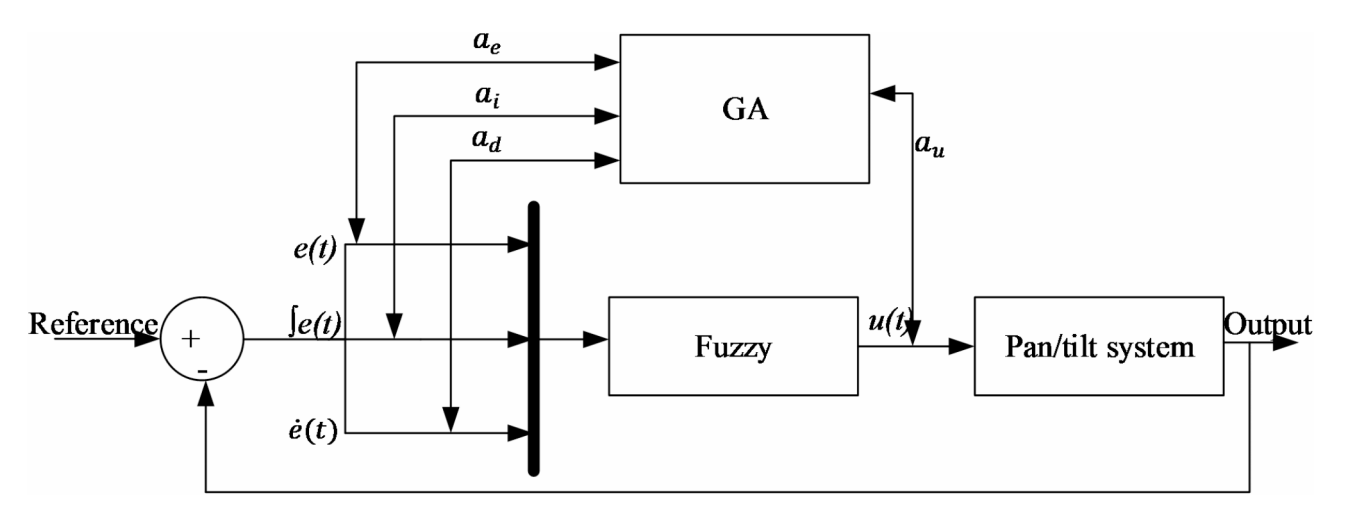


Fig. 8. The block diagram of optimal fuzzy PID controller.

The block diagram of the developed optimal Fuzzy-PID controller is given in Fig. 8 below.

The three inputs e(t), $\int e(t)$, $\dot{e}(t)$ and the output u(t) of the conventional PID controller are used as fuzzy variables in the fuzzy logic control design. The operating ranges for each of the variables are taken to be: $e(t) = [-a_e, a_e]$, $\int e(t) = [-a_i, a_i]$, $\dot{e}(t) = [-a_d, a_d]$, $u(t) = [-a_u, a_u]$.

For input fuzzy variables, each variable is represented by five triangular-shaped and equally spaced membership functions, and the output variable is represented by thirteen singleton membership functions. The fuzzy type used is Sugeno-type. The graphical definition of the membership functions is given in Fig. 9.

The overall fuzzy rules are represented by the sliced cube fuzzy associative memory (FAM)²⁹ as shown in Fig. 10. Each fuzzy rule is defined as:

If e(t) is E_i and $\int e(t)$ is I_j and $\dot{e}(t)$ is D_k THEN u(t) is U_l , l = i+j+k-2(26)

The crisp output, u(t), which is the corresponding equivalent fuzzy logic controller is given as follows^{29–33}:

$$u(t) = \frac{a_u}{3a_e} e(t) + \frac{a_u}{3a_i} \int e(t) dt + \frac{a_u}{3a_d} \dot{e}(t)$$
 (27)

Which gives us a linear PID controller with:

$$K_{P} = \frac{a_{u}}{3a_{e}}, K_{I} = \frac{a_{u}}{3a_{i}}, \text{ and } K_{D} = \frac{a_{u}}{3a_{d}}$$
 (28)

Our objective is to reduce the error between the object center and the camera center by designing Fuzzy Logic Control. we used error e(t) and change of error e(t) as input variables and control input u(t) as output variable to the controller. Five linguistic terms are assumed to be present for both the input and output variables in the present scenario. The linguistic terms for camera position in both x and y direction (pan and tilt motor) can be defined as Left (L), Left Center (LC), Center (C), Right Center (RC), Right (R), and Down (D), Down Center (DC), Center (C), Up Center (UC) and Up (U) respectively. It is possible to specify the appropriate output variable linguistic terms as NL (Negative Large), NS (Negative Small), Z (Zero), PS (Positive Small), and PL (Positive Large). Error Negative Large (ENA), Error Negative Small (ENB), Zero (Z), Error Positive Small (EPB), and Error Positive Large (EPA). The numerical functions corresponding to each linguistic term have been created by applying the normalized standard membership functions (Triangular Type and Trapezoidal Type) and illustrated in the following Fig. 11a-c.

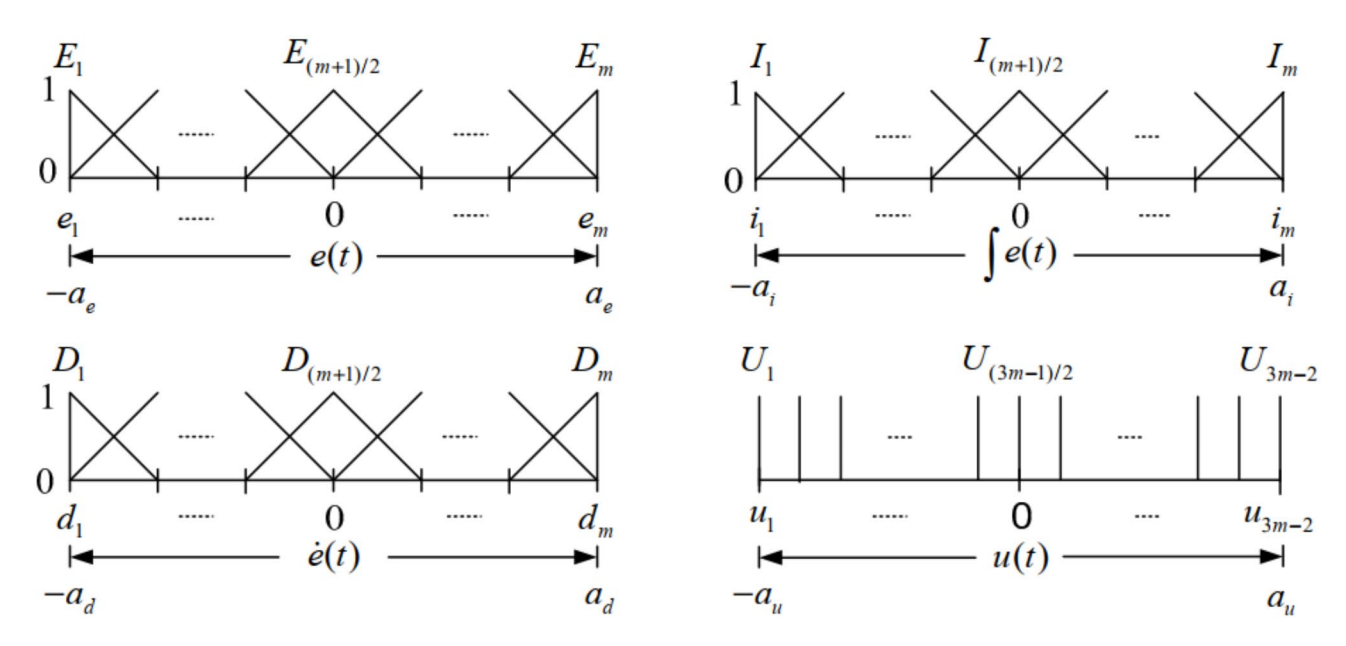


Fig. 9. Definition of membership functions for fuzzy variables²⁹.

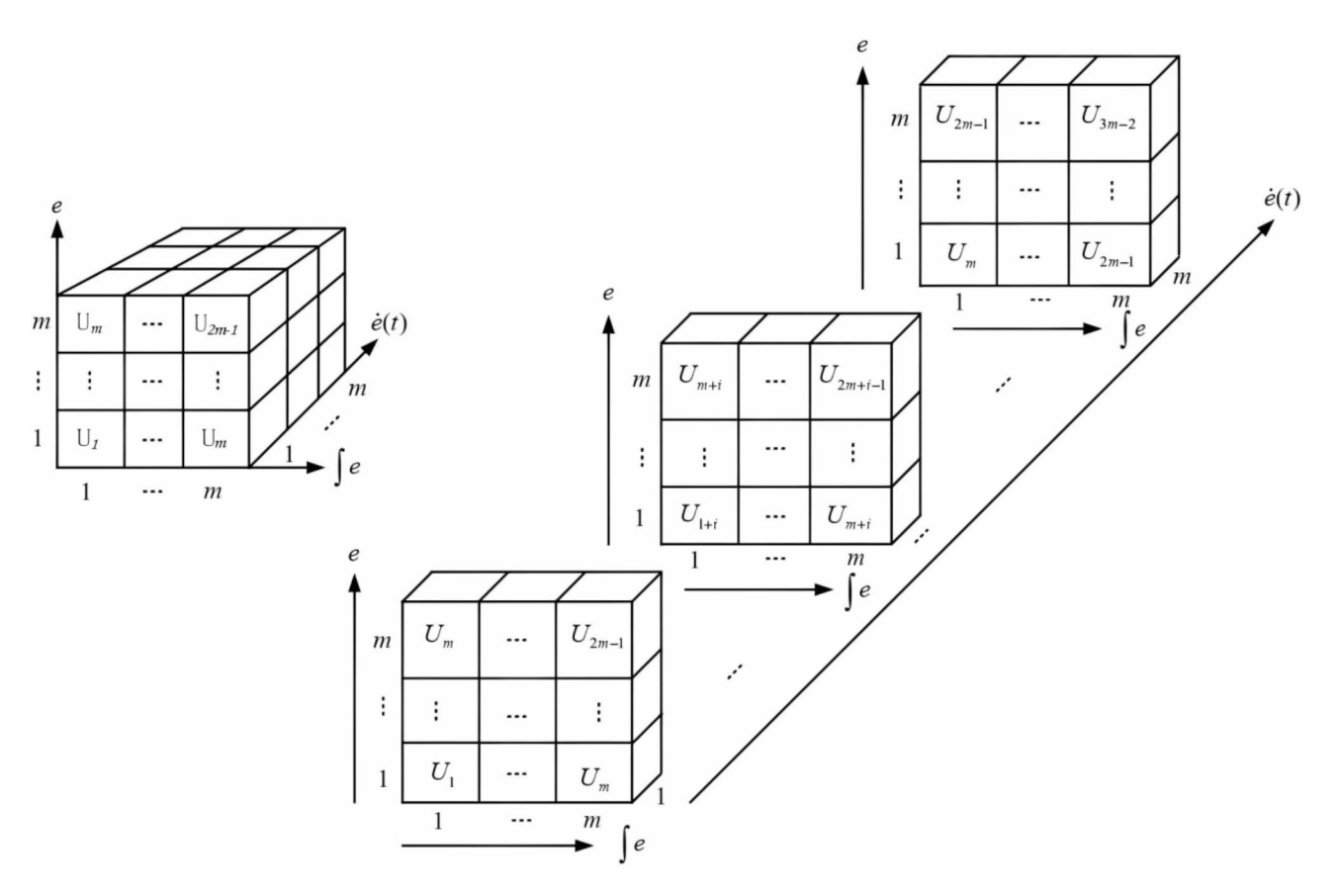


Fig. 10. Sliced cube FAM representation of the knowledge base²⁹.

The Fuzzy Logic IF-THEN rule base was carefully created for this study in order to relate the input variables to the intended control output. The error and the change in error are the inputs to the fuzzy logic system (FLS), and both are essential for capturing the system's dynamic behavior. The control signal, which is the FLS's output, adjusts the system to operate as intended. The Fuzzy Logic IF-THEN Rule Base consists of a set of linguistic if-then rules that define the relationship between the inputs and the output as shown in Table 3.



Fig. 11. Membership functions of pan and tilt motor; (a) error, (b) change of error and (c) output.

Considering all the available fuzzy inference methods, the AND (Minimum) antecedent connective was selected for this work, as it provided better results in terms of system performance. This method ensures that the degree of membership for the antecedents is calculated as the minimum value, leading to a more precise evaluation of the rule activation strength.

		Change of error				
AND		ENA	ENB	Z	EPB	EPA
Error	L	NL	NL	NS	NS	PL
	LC	NS	NS	NS	NS	PS
	С	Z	NS	Z	Z	Z
	RC	PS	Z	PS	NS	NS
	R	PL	PS	PS	NS	NL

Table 3. A complete rule base used in this work.

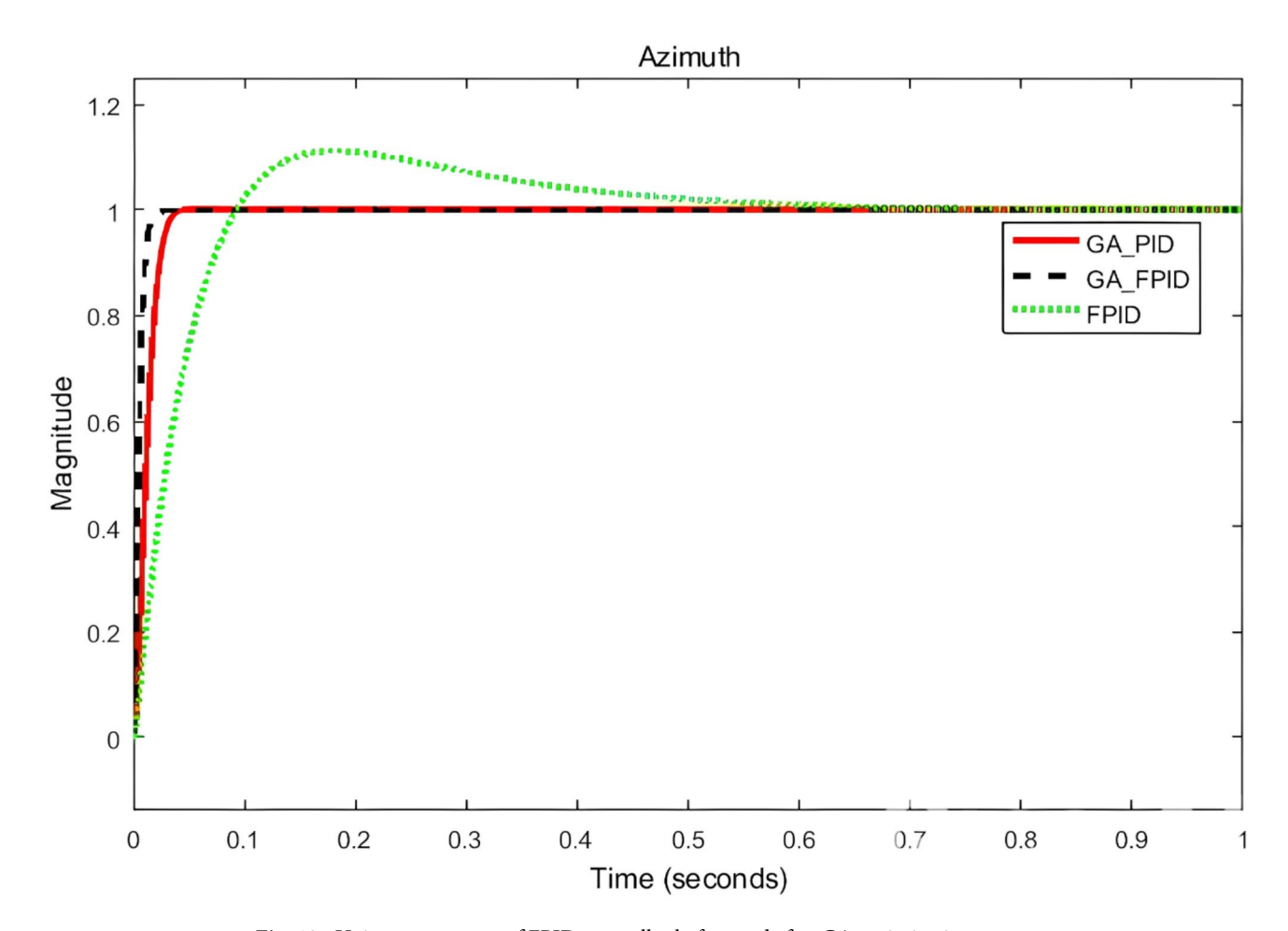


Fig. 12. Unit step response of FPID controller before and after GA optimization.

Results and discussion

Object tracking is a complex task involving various interconnected components. This paper focuses on developing a 2-dimensional (2D) object tracker that functions effectively with both static and dynamic cameras. Our primary goal is to achieve efficient camera movements while maintaining accurate tracking. The performance assessment of the designed controllers is provided in the first section. The static camera-based object tracking is presented next. Lastly, object tracking using a dynamic camera is demonstrated.

Performance evaluation

The performance of Fuzzy-PID, GA tuned PID and GA tuned Fuzzy-PID controllers are evaluated in tracking. Due to symmetry, the response of the pan actuator is presented and analyzed. The output response obtained before and after using GA optimization for Fuzzy-PID and PID controller are shown in Fig. 12. As shown in the figure the un tuned Fuzzy-PID controller has maximum overshoot, large settling time and rise time. While the GA tuned PID and Fuzzy-PID controller show better results in reduced rise and settling time, and zero overshoot. The corresponding transient and steady-state parameters are as tabulated in Table 4.

As shown in Table 4, the GA-tuned FPID controller had given comparatively better results over the GA-tuned PID controller. The rise time reduced from 20.2 to 9.4 milliseconds (ms). The settling time is dropped from 34

	Transient and steady-state response parameter (Pan)				
Controller	T _r (ms)10-90%	T_s (ms) \pm 2%	Steady-state error	Overshoot (%)	
GA_FPID	9.4	16	3.973* 10 ⁻⁵	0	
GA_PID	20.2	34	6.775* 10 ⁻⁵	0.1	
FPID	65.6	500	7.130* 10 ⁻⁴	11.2	

Table 4. Transient and steady-state response parameters for azimuth.

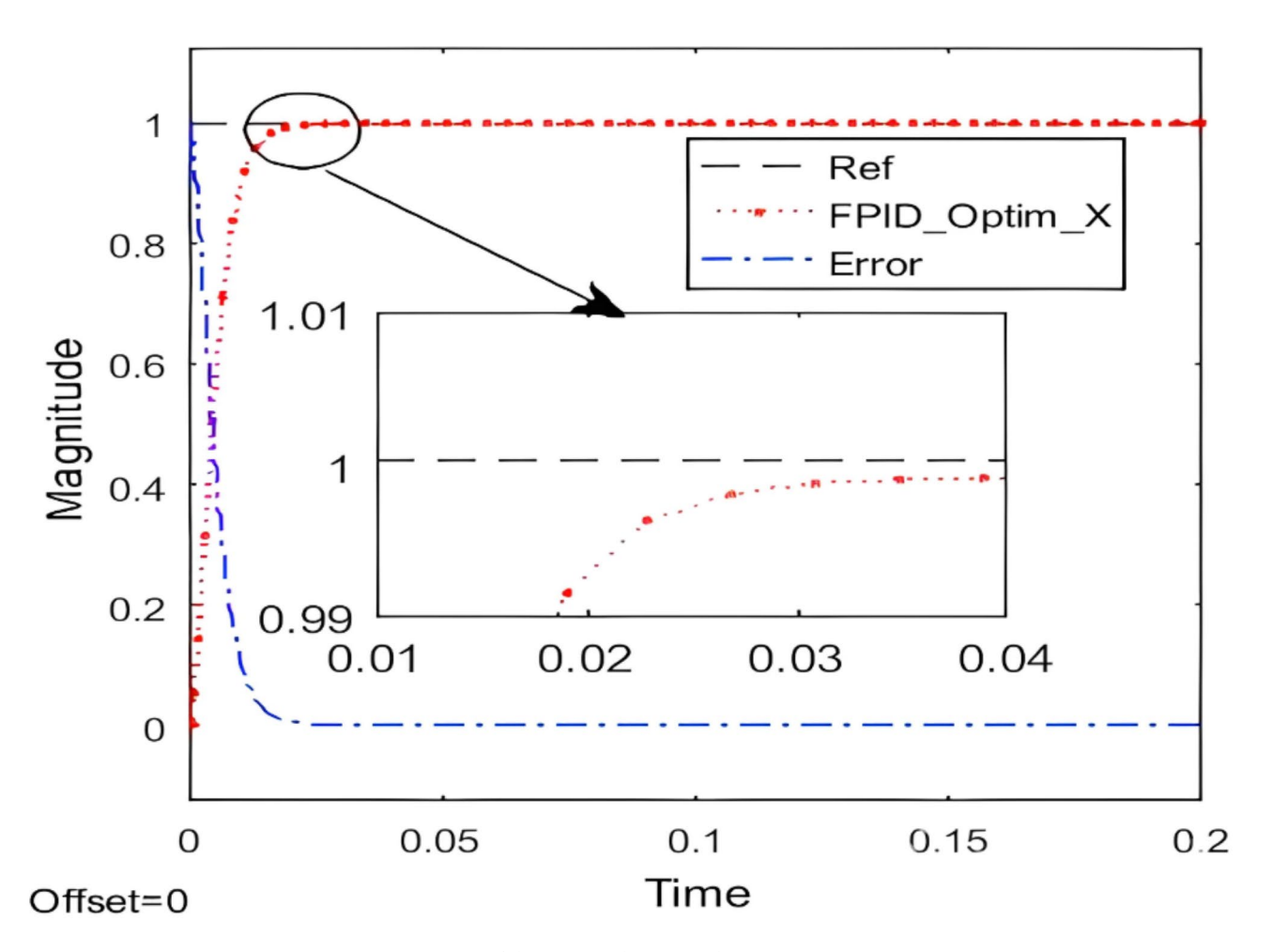


Fig. 13. Unit step response of the proposed GA tuned FPID system.

Parameter			_		-
Azimuth	3.01	108.91	759.64	4752.19	3169.12

Table 5. Tuned FPID controller parameters.

to 16 milliseconds (ms). The steady-state error is negligible for each case and the maximum overshoot has been reduced from 11.2 to 0.1 and 0 for GA PID and GA FPID controllers respectively for pan motor.

Figure 13 presents a zoomed view of the Fuzzy-PID controller's response after being tuned with GA. The graph also shows the corresponding error signal. Compared to the reference signal (desired response), the optimized Fuzzy-PID controller exhibits minimal oscillation and achieves a near-zero steady-state error. This indicates excellent tracking performance.

Table 5 shows the specific values (k1-k5) for the gain parameters after tuning. It's important to note that some of these values might appear quite large. This is because achieving a fast system response often requires the controller to utilize a high amount of energy. Consequently, the tuned system will consume more energy

compared to the un tuned one. This trade-off between fast response and energy efficiency is a common challenge in control system design.

The actuating signals for the controllers are given in Fig. 14. As shown, the control voltage in case of GA tuned Fuzzy-PID controller is big, which may go beyond the ratings of our actuators used and may tend them to damage. To overcome this limitation, a saturation is employed which prevents the actuator's voltage from exceeding its rated maximum.

Figure 15 shows the response of the actuating signal to a step input with saturation applied. The system achieves a steady-state error of $3.095 \times 10^*$ -3 while keeping the actuating signal at its maximum rated value of 24 V, which is the actuator's limit.

As stated above the ITAE is used as a performance measure. The cost function for the GA is used from this ITAE. As the number of iterations increase, the cost function converges to zero. For our case the ITAE fitness function after 30 iterations is given by Fig. 16. Its value is about 0.00159261, which converges to zero.

External disturbance rejection capability

The performance of the controllers with external disturbance are tested by additively applying a pulse signal of amplitude 2, frequency 1 rad/sec and pulse width of 10% at the input to the system. Due to symmetry only the controllers of the azimuth motor are discussed here. The performance of the design controller with an external disturbance like wind and dust is shown in the below figure. As the simulation results showed the GA tuned Fuzzy-PID controller has a better performance.

The robustness of the controllers in handling external disturbances was evaluated by injecting a pulse signal into the system's input. This pulse disturbance mimicked real-world challenges by having an amplitude of 2, a frequency of 1 rad/sec, and a pulse width of 10%. Figure 17 illustrates the response of the designed controller, specifically a GA-tuned Fuzzy-PID controller, when subjected to these external disturbances resembling wind and dust. As evident from the simulation results, the GA-tuned Fuzzy-PID controller exhibited superior performance in maintaining system stability and accuracy compared to other controllers tested. This highlights the effectiveness of the Fuzzy-PID control strategy, particularly when fine-tuned with a Genetic Algorithm, in mitigating the impact of external factors on the system's performance.

Static camera

The interest object has been tracked with a static camera. The block diagram has been constructed in LabVIEW with vision acquisition and vision assistant tools. While doing image processing, the interest object's kernel has been selected and for the purpose of increased efficiency, the gray-scale was used over RGB. When it gets matched to the previously stored template, the object found button is on, and the new captured object has been tracked. The kernel was saved as a template and the new object has been compared to it. When it gets matched to

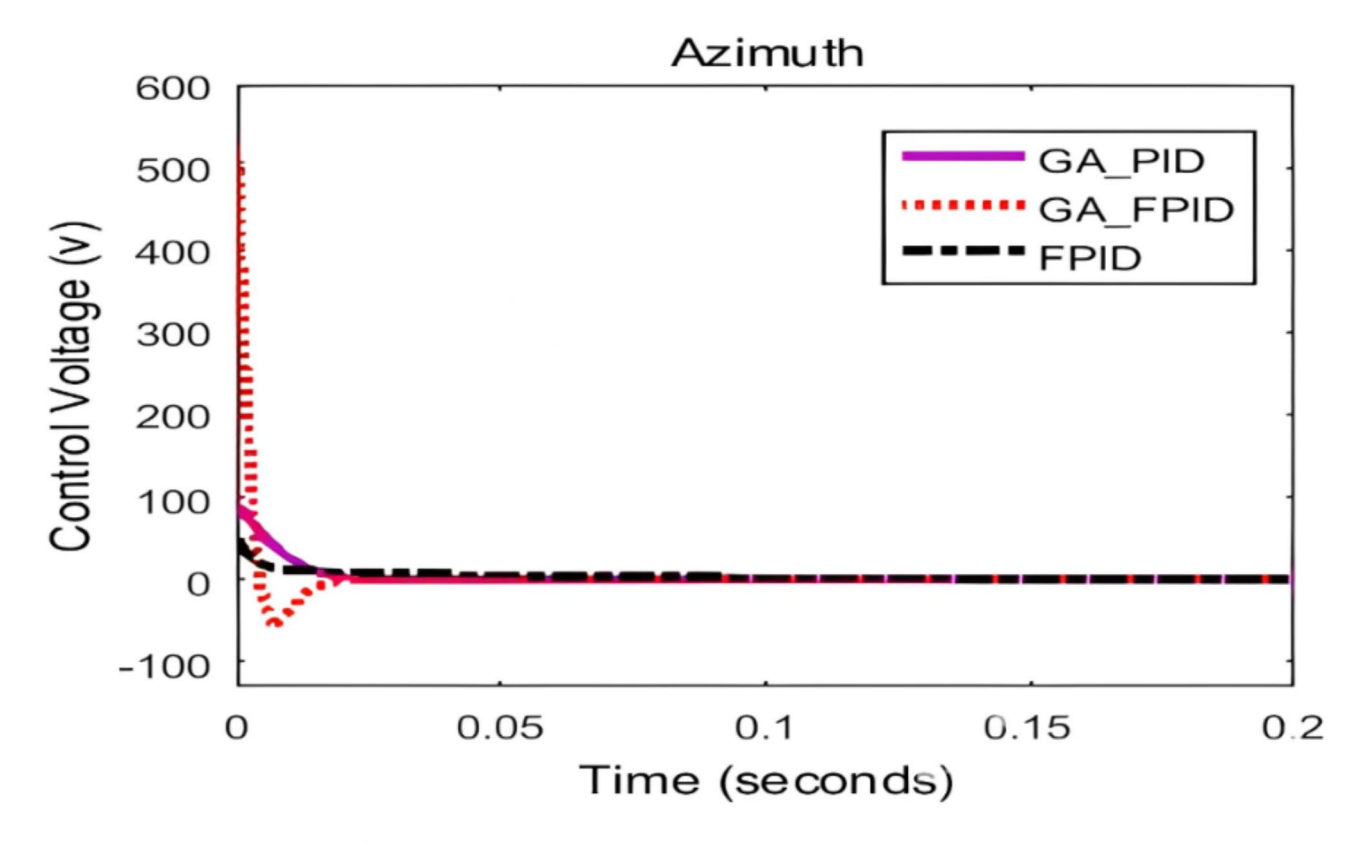


Fig. 14. The actuating signals due to a step input.

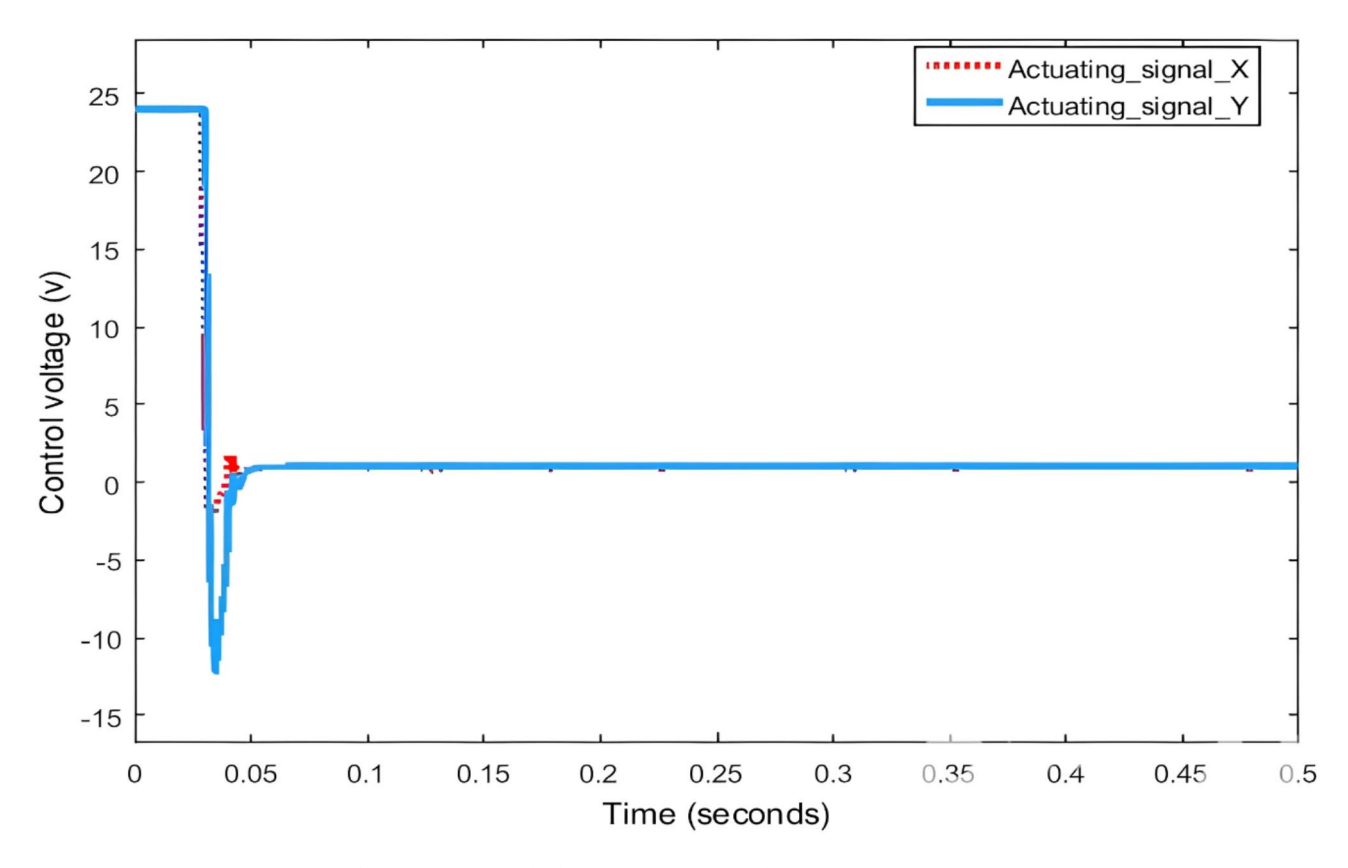


Fig. 15. The actuating signals due to a step input with saturation.

the previously stored template, the object found button is on, and the new captured object has been tracked. The motion of the object has been tracked by integrating the math script node and LabVIEW blocks.

In Fig. 18, a random trajectory of the object in real time is taken and has been sketched just to show that the camera has detected and followed the path of the object it follows.

Dynamic camera

The drawback of static camera-based object tracking is that the field of view is fixed and the object is lost if it goes out of the focus area of the camera. To overcome this problem the camera is then attached to a pan/tilt mechanism and let to pan and tilt in the 2-D plane. Object loss near the boundaries of a camera's field of view can be successfully minimized with a dynamic camera system that incorporates a pan/tilt mechanism. This system dynamically modifies the camera's angle to maintain objects inside view by using real-time object detection to identify objects approaching its' boundaries.

A sinusoidal trajectory of amplitude 1 and angular frequency 1 rad/sec, 50 rad/sec and 100 rad/sec are taken as a reference signal to show the performance of the object tracking capability of the camera. The time response plots are given in Fig. 19. As shown from the given plots, the sinusoidal trajectory generated is tracked with negligible steady-state error at 1 rad/sec and the steady-state error increases at high frequencies. The designed controller has tracked the reference trajectories at low frequencies. NB: due to symmetry, the response results of the pan actuator are put here.

Responses of Fig. 19b & c demonstrate a clear trend, as the input frequency increases, the steady state error rises progressively. This behavior aligns with real-world systems, where tracking accuracy often diminishes with higher frequency inputs. At a frequency of 100 rad/sec (Fig. 19c), the steady-state error becomes significant, as evident from the figure. Response shown in Fig. 19b, with a frequency of 50 rad/sec, exhibits an intermediate performance better than Fig. 19c but inferior to the low-frequency response of Fig. 19a which is 1 rad/sec.

To further evaluate the pan-tilt mechanism's trajectory tracking prowess, the system was subjected to reference signals representing circular and elliptical paths. These tests aimed to assess the mechanism's ability to follow predefined, curved paths. As depicted in Figs. 20 and 21, the simulation results were promising at low frequencies (0.5 rad/sec and 1 rad/sec). At 0.5 rad/sec, the pan-tilt mechanism precisely followed the designated circular or elliptical trajectory, exhibiting minimal steady-state error. This indicates excellent tracking accuracy at slower speeds. However, as the frequency increased to 1 rad/sec, a noticeable error became evident in the tracking response. This suggests that the mechanism's ability to perfectly adhere to the desired path diminishes at higher speeds.

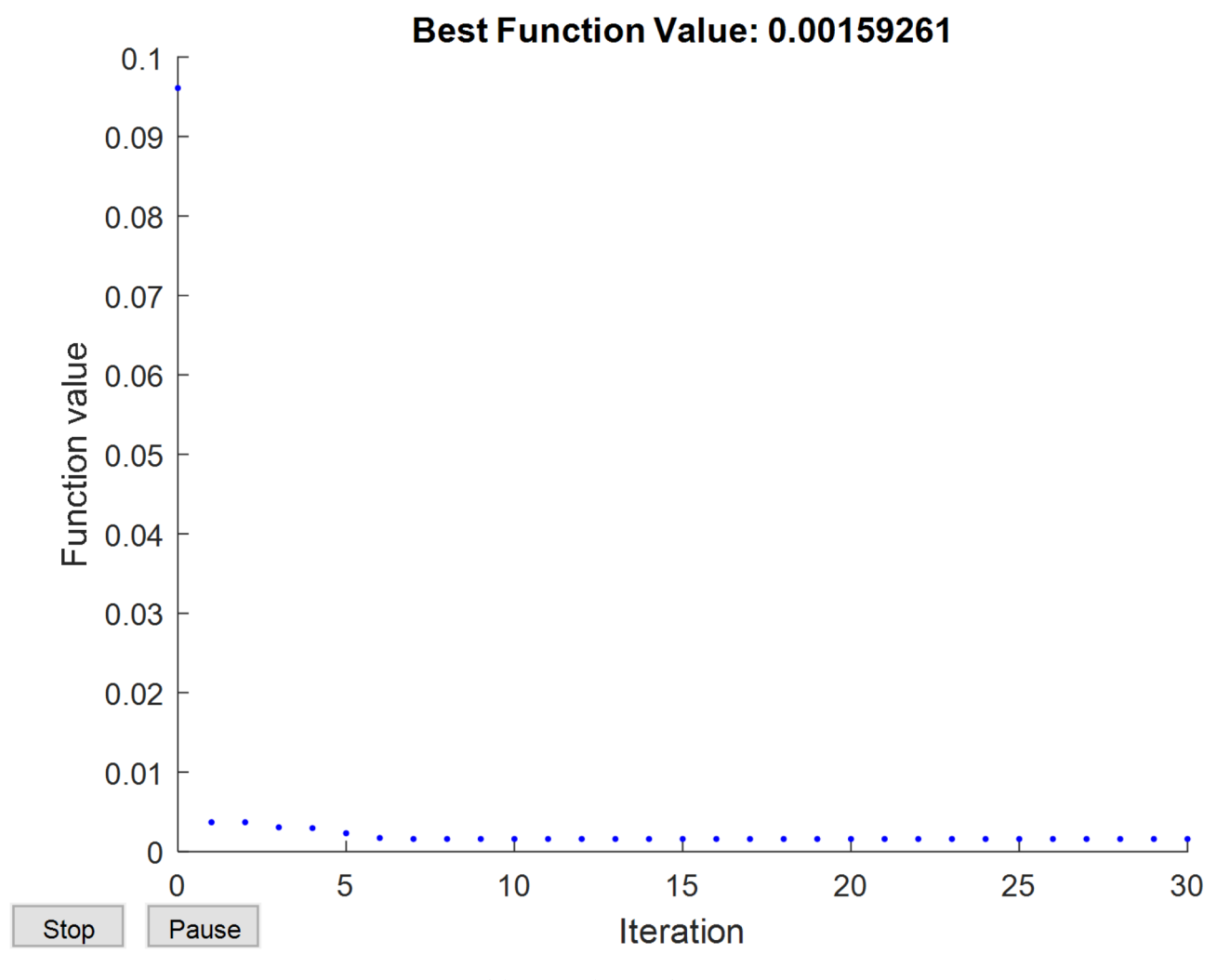


Fig. 16. Convergence curve of the ITAE objective function.

Conclusion and future work Conclusion

This work successfully addressed object detection and tracking within a computer vision system. NI-LabVIEW facilitated object detection and static camera-based object tracking. However, for dynamic camera scenarios, a more robust approach was required. To this end, the paper introduced an optimal Fuzzy-PID controller. This controller merges the strengths of conventional PID control with fuzzy logic, enabling it to effectively handle the non-linearities inherent in dynamic camera tracking systems.

The operating ranges (scaling factors) of the membership functions of the fuzzy variables, which define the controller's behavior, were optimized using GA. This optimization ensured the controller was specifically tailored to the non-linearities of the tracking system. Simulation results convincingly demonstrated that the optimal Fuzzy-PID controller significantly outperformed conventional PID, fuzzy-only, and even basic Fuzzy-PID controllers.

Furthermore, the paper investigated the controller's performance under disturbance and varying frequencies. As expected, the results revealed a decrease in system performance with increasing frequency. This is because higher frequencies introduce more rapid changes, which can be more challenging for the controller to manage.

Overall, this work presents a novel and effective approach to object tracking in dynamic camera scenarios. The optimal Fuzzy-PID controller offers a significant improvement over traditional methods by effectively handling non-linearities and disturbances.

Future work

In the future further research can be conducted in the application of GA in the object detection phase, in optimizing the non-linear factors of a membership function and the rule bases. In addition to this a novel solution will be proposed by the employment of new controllers based on neural networks as well as a more efficient analysis of what has been achieved to date. Moreover, we want to stress that using other optimization technique such as particle swarm optimization (PSO), simulated annealing (SA) and Swarm Intelligence-Based

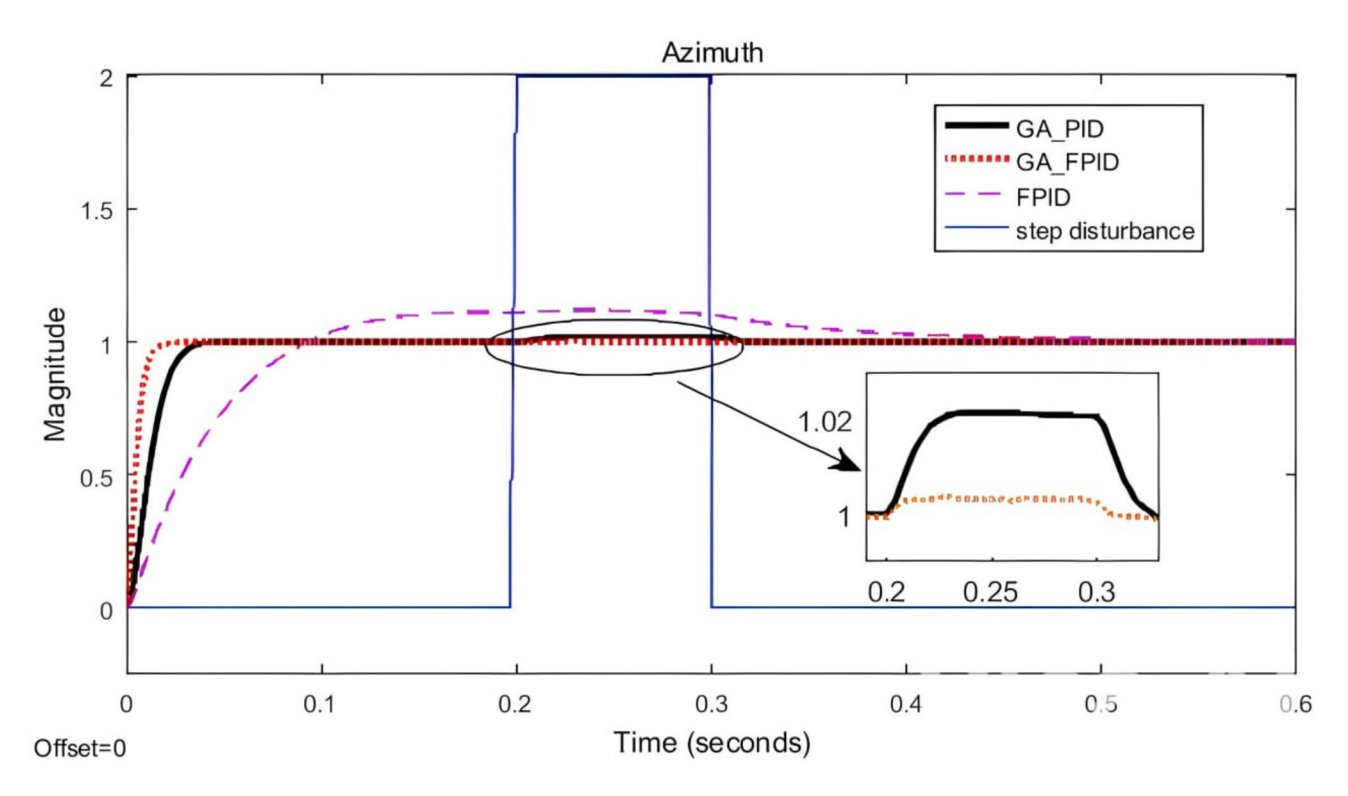


Fig. 17. External disturbance rejection capability of the controller.

Methods may use as an alternative optimization technique for comparison. We also recommend practical implementation of this work in the future.

Future research will concentrate on verifying the simulation results with experimental data, even if this study offers insightful information through simulation-based analysis. Real-world data collection or physical experimentation will allow for a more thorough assessment of the suggested strategy and its usefulness. In order to compare and assess any disparities and adjust the methods appropriately, this will entail creating and putting into place an experimental setup that closely resembles the simulation environment. By including experimental validation, the results will be more robust and applicability to real-world scenarios will be further supported. We also suggest a thorough examination of the system's limitations at higher frequencies, with particular attention to the controller's response time and the hardware and sensor dynamic limitations.

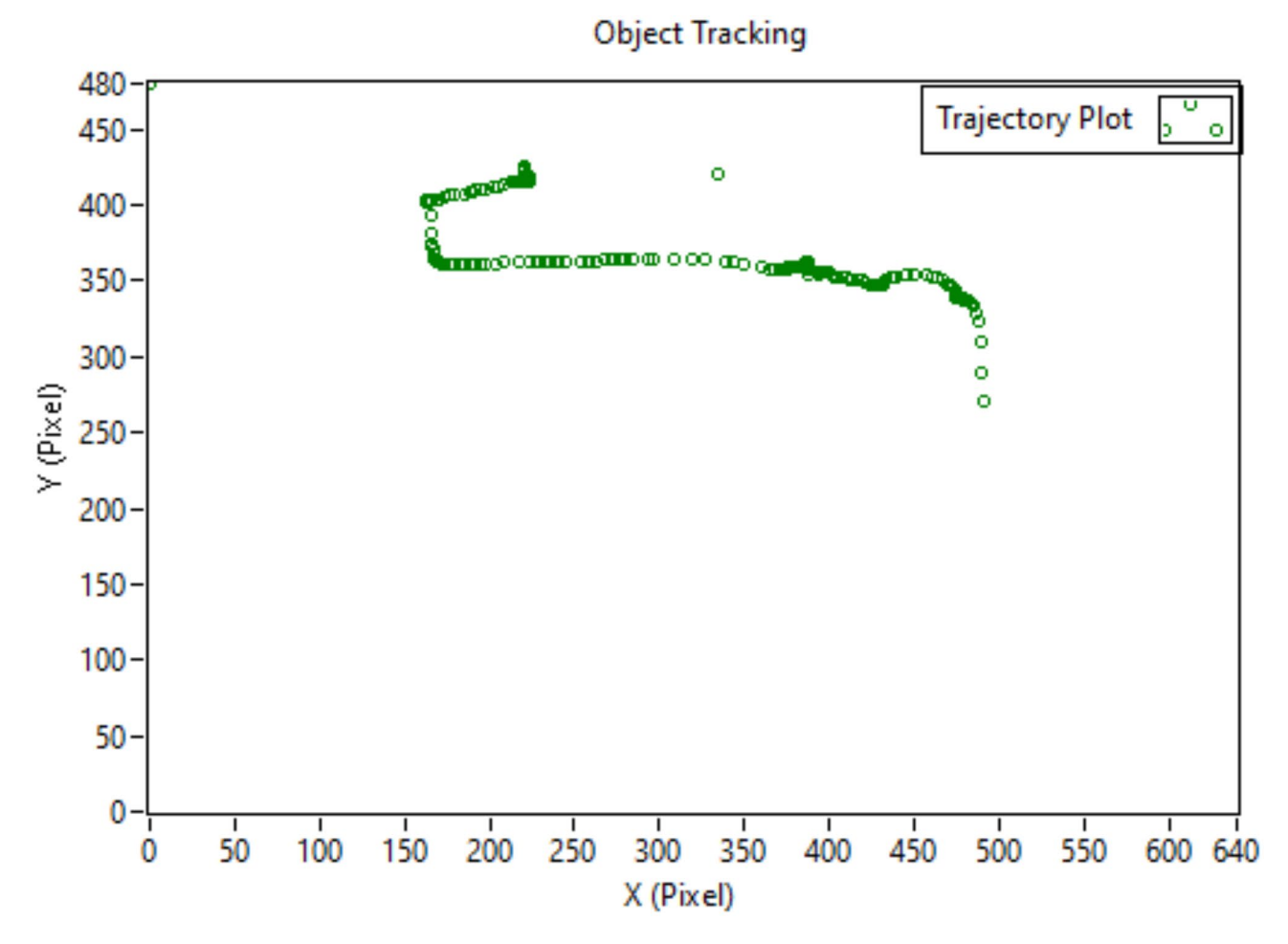


Fig. 18. Interest object trajectory plot.

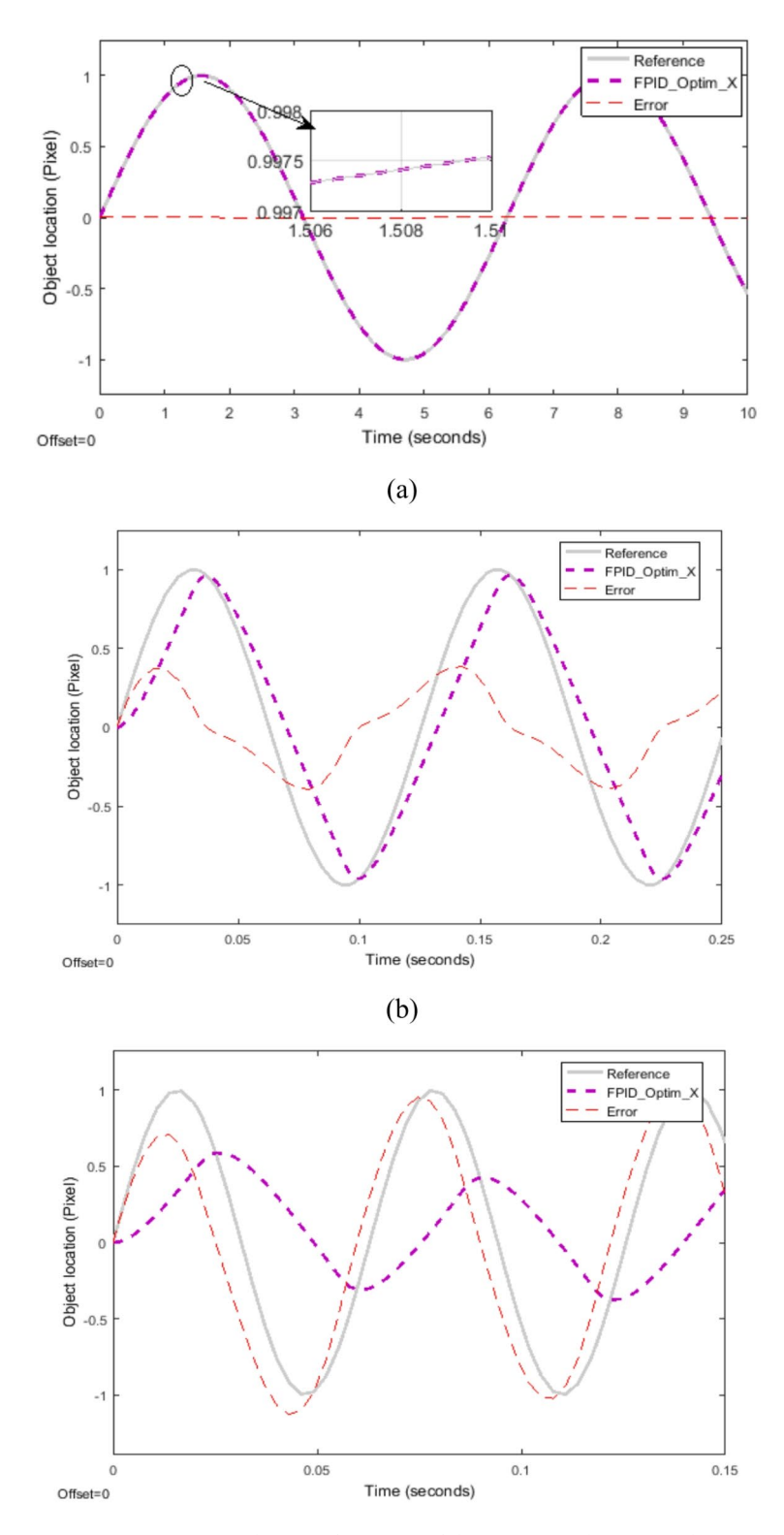


Fig. 19. Trajectory tracking performance of the camera with GA tuned FPID Controller (a) at 1 rad/sec (b) at 50 rad/sec and (c) at 100 rad/sec.

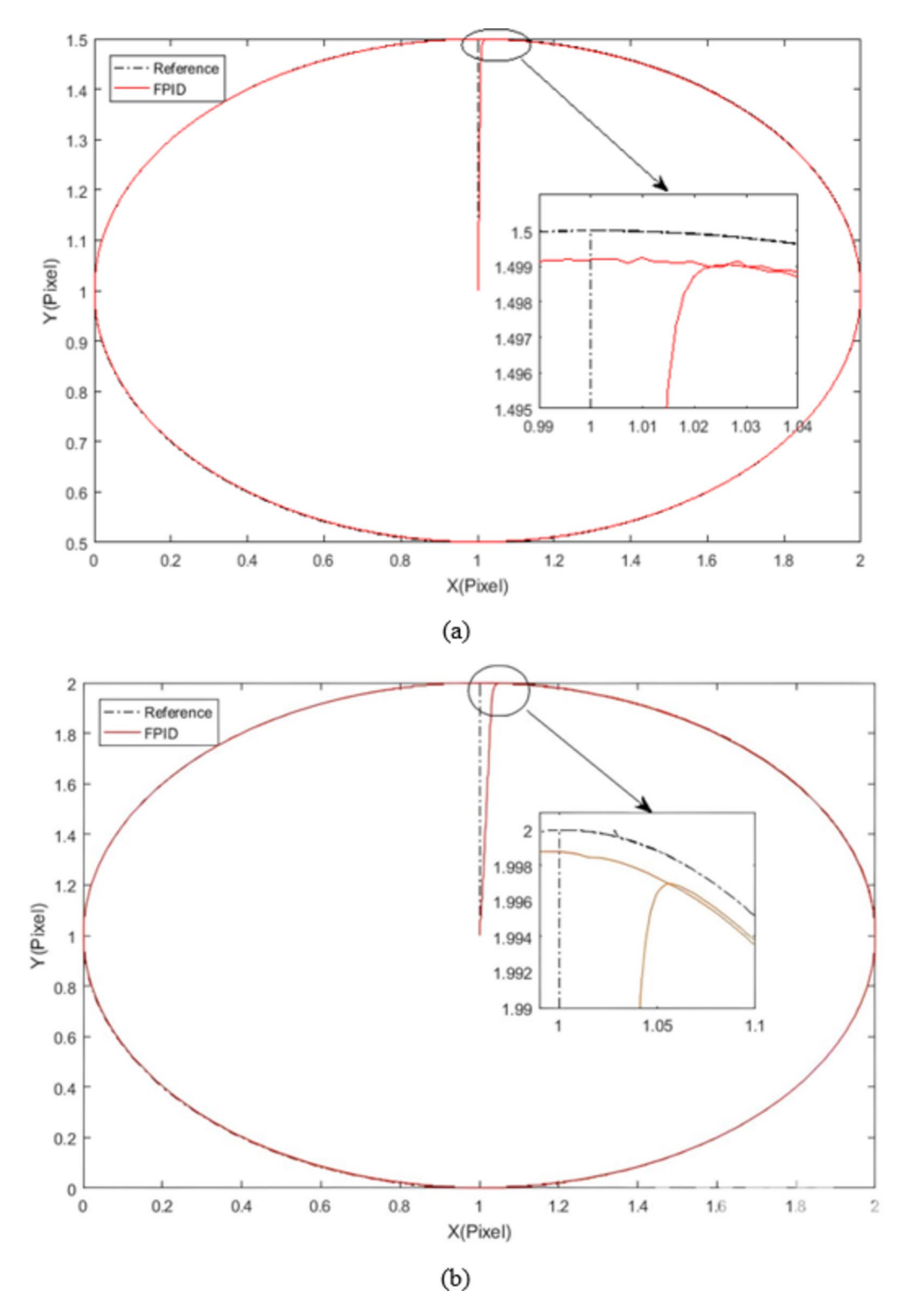


Fig. 20. Circular trajectory tracking capability of the pan/tilt system (a) 0.5 rad/sec and (b) 1 rad/sec.

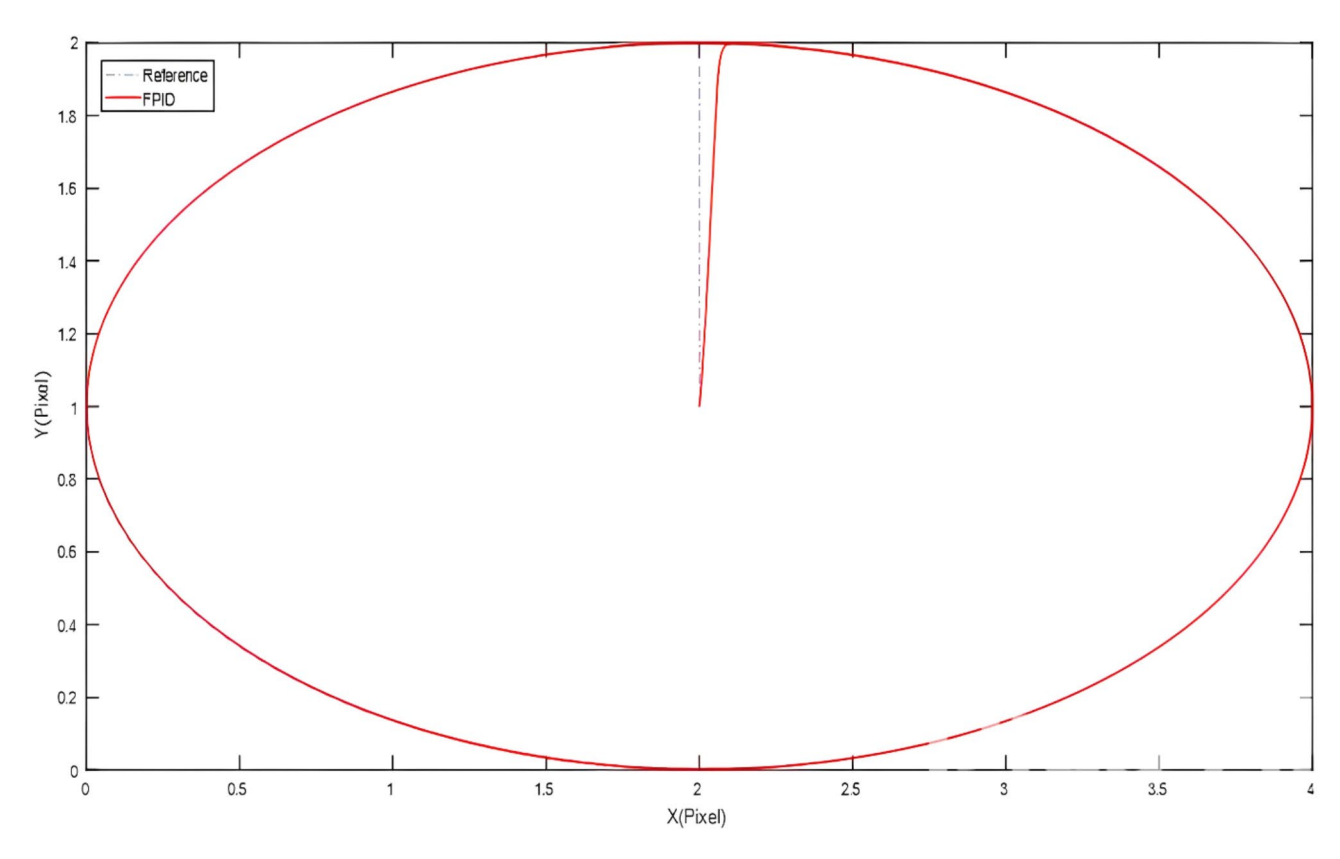


Fig. 21. Elliptical trajectory tracking capability of the pan/tilt system at 1 rad/sec.

Data availability

The datasets used and/or analyzed during the current study available from the corresponding author on reasonable request.

Received: 7 October 2024; Accepted: 26 February 2025

Published online: 08 April 2025

References

- 1. Lopes, N. M. L. V. Fuzzy logic based approach for object feature tracking (Universidade de Tras-os-Montes e Alto Douro (Portugal), 2011).
- Gururaj, M. S., Ramesh, M. H. & Arvind, J. A. A review on image tracking technique in Labview. Int. J. Sci. Dev. Res. 1, 90–92 (2016).
- 3. Rout, R. K. A survey on object detection and tracking algorithms, Depart. Computer Sci. Eng. Nat. Instit. Technol. Rourkela Rourkela-769 8, (2013).
- 4. Zou, Z., Chen, K., Shi, Z., Guo, Y. & Ye, J. Object detection in 20 years: A survey, Proceedings of the IEEE, 111, 257-276, (2023).
- 5. Divya, M. & Ravi Kumar, A. Single object tracking system by using Labview. *Int. J. Recent. Innov. Trends Comput. Commun..* 4, 52–56 (2016).
- Chulakit, S. et al. A webcam and LabVIEW-based system for efficient object recognition based on colour and shape features. J. Adv. Res. Appl. Mech. 104, 33–45 (2023).
- Mokhtari, M. A. & Taheri, M. Real-time object detection and tracking using YOLOv3 network by quadcopter. Mech. Based Des. Struct. Mach., pp. 1–19, (2022).
- 8. He, L. Detection-assisted object tracking by ,mobile cameras, (2011).
- 9. Wu, Z. & Wang, F. Surface irrigation based on image object detection and fuzzy Pid control. Arab. J. Geosci., 14, (2021).
- 10. Mehrubeoglu, M., Pham, L. M., Le, H. T., Muddu, R. & Ryu, D. Real-time eye tracking using a smart camera, in 2011 IEEE Applied Imagery Pattern Recognition Workshop (AIPR), pp. 1–7. (2011).
- 11. Wang, P. S., Lin, C. H. & Chuang, C. T. Real-time object localization using a fuzzy controller for a vision-based drone, *Inventions*, 9, p. 14, (2024).
- 12. Amirkhani, A., Shirzadeh, M., Kumbasar, T. & Mashadi, B. A framework for designing cognitive trajectory controllers using genetically evolved interval type-2 fuzzy cognitive maps. *Int. J. Intell. Syst.* 37, 305–335 (2022).
- 13. Venu, D. Object detection in motion estimation and tracking analysis for IoT devices. Eur. Chem. Bull. 12, 236-255 (2023).
- 14. Biyyapu, V., Reddy, Y. V., Reddy, S. K. & Priyadarshini, P. Object detection using OpenCV, in AIP Conference Proceedings, (2024).
- Zhang, S. X., Zhu, X., Hou, J. B. & Yin, X. C. Graph fusion network for multi-oriented object detection. Appl. Intell. 53, 2280–2294 (2023).
- Jahedi, G. & Ardehali, M. Genetic algorithm-based fuzzy-PID control methodologies for enhancement of energy efficiency of a dynamic energy system. Energy. Conv. Manag. 52, 725–732 (2011).
- 17. Ekinci, S., Izci, D., Eker, E. & Abualigah, L. An effective control design approach based on novel enhanced aquila optimizer for automatic voltage regulator. *Artif. Intell. Rev.* **56**, 1731–1762 (2023).

- 18. Izci, D., Hekimoğlu, B. & Ekinci, S. A new artificial ecosystem-based optimization integrated with Nelder-Mead method for PID controller design of Buck converter. *Alexandria Eng. J.* **61**, 2030–2044 (2022).
- 19. Izci, D., Ekinci, S. & Hussien, A. G. Effective PID controller design using a novel hybrid algorithm for high order systems. *PLoS One.* 18, e0286060 (2023).
- 20. Izci, D., Ekinci, S., Eker, E. & Kayri, M. Augmented hunger games search algorithm using logarithmic spiral opposition-based learning for function optimization and controller design. *J. King Saud Univ. Eng. Sci.*, (2022).
- 21. Amirkhani, A., Shirzadeh, M. & Molaie, M. An indirect type-2 fuzzy neural network optimized by the grasshopper algorithm for vehicle ABS controller. *IEEE Access.* 10, 58736–58751 (2022).
- 22. Shirzadeh, M., Amirkhani, A., Tork, N. & Taghavifar, H. Trajectory tracking of a quadrotor using a robust adaptive type-2 fuzzy neural controller optimized by cuckoo algorithm. ISA Trans. 114, 171–190 (2021).
- 23. Izci, D. & Ekinci, S. A novel improved version of hunger games search algorithm for function optimization and efficient controller design of buck converter system, e-Prime-Adv. Electrical Eng. Electron. Energy, 2, 100039, (2022).
- 24. Kye-Si, K. & S. READY and Practical guide to machine vision software: an introduction with labVIEW (Wiley-VCH, 2015).
- 25. Jinlong, E., He, L., Li, Z. & Liu, Y. WiseCam: wisely tuning wireless pan-tilt cameras for cost-effective moving object tracking, in *IEEE INFOCOM 2023-IEEE Conference on Computer Communications*, 1–10. (2023).
- Manuel, N. L., İnanç, N. & Lüy, M. Control and performance analyses of a DC motor using optimized PIDs and fuzzy logic controller. Results Control Optim. 13, 100306 (2023).
- 27. Samuel, E. S. Neuro-fuzzy based approach to object tracking and motion prediction Ed (IJSEA, 2017).
- 28. Firoozian, R. Servo motors and industrial control theory (Springer, 2014).
- 29. Chao, C. T., Sutarna, N., Chiou, J. S. & Wang, C. J. An optimal fuzzy PID controller design based on conventional PID control and nonlinear factors, *Appl. Sci.*, **9**,1224, (2019).
- Rabah, M., Rohan, A., Han, Y. J. & Kim, S. H. Design of fuzzy-PID controller for quadcopter trajectory-tracking. Int. J. Fuzzy Log. Intell. Syst. 18, 204–213 (2018).
- 31. Rodríguez-Abreo, O., Rodríguez-Reséndiz, J. & García-Cerezo, A. and J. R. García-Martínez, Fuzzy logic controller for UAV with gains optimized via genetic algorithm, *Heliyon*, (2024).
- 32. Saxena, A., Sharma, K., Kadirgama, K., Devarajan, R. & Noor, M. Comparative performance evaluation of PID and fuzzy PID controller using genetic algorithm for a robotic manipulator system, in AIP Conference Proceedings, (2024).
- 33. Liu, J., Wu, X., Quan, L., Xu, H. & Hua, Y. Fuzzy adaptive PID control for path tracking of field intelligent weeding machine. *AIP Adv.*, **14**, (2024).

Author contributions

Yaregal Limenih Melese: Conceptualization, Methodology, Software, Visualization, Writing – original draft, Validation. Girma Kassa Alitasb: Investigation, Data curation, Methodology, Software, Writing –review & editing, Validation. Mequanent Degu Belete: Investigation, Data curation, Software, Writing –review & editing, Validation.

Declarations

Competing interests

The authors declare no competing interests.

Additional information

Correspondence and requests for materials should be addressed to G.K.A.

Reprints and permissions information is available at www.nature.com/reprints.

Publisher's note Springer Nature remains neutral with regard to jurisdictional claims in published maps and institutional affiliations.

Open Access This article is licensed under a Creative Commons Attribution-NonCommercial-NoDerivatives 4.0 International License, which permits any non-commercial use, sharing, distribution and reproduction in any medium or format, as long as you give appropriate credit to the original author(s) and the source, provide a link to the Creative Commons licence, and indicate if you modified the licensed material. You do not have permission under this licence to share adapted material derived from this article or parts of it. The images or other third party material in this article are included in the article's Creative Commons licence, unless indicated otherwise in a credit line to the material. If material is not included in the article's Creative Commons licence and your intended use is not permitted by statutory regulation or exceeds the permitted use, you will need to obtain permission directly from the copyright holder. To view a copy of this licence, visit https://creativecommons.org/licenses/by-nc-nd/4.0/.

© The Author(s) 2025